Structural Depinning of Ne Monolayers on Pb at $T < 6.5$ K

L. Bruschi, G. Fois, A. Pontarollo, and G. Mistura
Dipartimento di Fisica G. Galilei, Università di Padova, via Marzolo 8, 35131 Padova, Italy

B. Torre, F. Buatier de Mongeot, C. Boragno, R. Buzio, and U. Valbusa
Dipartimento di Fisica, Università di Genova, via Dodecaneso 33, 16146 Genova, Italy
(Received 25 January 2006; published 30 May 2006)

We have studied the nanofriction of Ne monolayers with a quartz-crystal microbalance technique at temperatures below 6.5 K and in ultrahigh-vacuum conditions. Very homogeneous and smooth lead electrodes have been physically deposited on a quartz blank at 150 K and then annealed at room temperatures. With such a Pb-plated quartz-crystal microbalance, we have observed a pronounced depinning transition separating a low-coverage region, where the film is nearly locked to the oscillating electrode, from a high-coverage region characterized by slippage at the solid-fluid boundary. Such a behavior has been found to be very reproducible. These data are suggestive of a structural depinning of the solid Ne film when it becomes incommensurate with the lead substrate, in agreement with the results of an extensive molecular-dynamics study.

DOI: 10.1103/PhysRevLett.96.216101 PACS numbers: 68.35.Af, 67.70.+n, 68.55.−a, 68.60.−p

One of the most serious problems holding back the development of a variety of microelectromechanical systems (MEMS) devices that could form the building blocks for more sophisticated on-chip systems is friction and wear at the dry interface [1,2]. These severe limitations cannot be solved by simply adding traditional lubricants, because these MEMS structures collapse to capillary forces in the presence of liquids. Recent results in the study of dry friction may suggest new strategies to tackle such problems.

In fact, the friction between two solid bodies in contact may assume very small values when the two crystalline surfaces are incommensurate [3], a phenomenon emphatically called superlubricity. The underlying idea is that the force coming from the mismatched atoms in the contact area point in all directions and sum up to zero. Vanishing friction on a silicon surface was observed with ultrahigh-vacuum (UHV) scanning tunneling microscopy [4]. More recently, the energy dissipation between a graphite flake sliding over a highly oriented pyrolitic graphite substrate in dry contact has been studied with a very sensitive frictional force microscope [5]. It was found that friction was significantly reduced when the two graphite surfaces are rotated out of the commensurate locking angle. In another study, the friction between a tungsten tip moving on a NaCl crystal was measured under UHV conditions as a function of the normal load applied to the tip [6]. A transition from stick-slip to continuous sliding was reported. When the stick-slip instabilities ceased to exist, a new regime of ultralow friction was encountered that can be explained with a concept similar to that mentioned above for an incommensurate contact. Negative and positive lateral forces sum up to a vanishing force in the time average rather than the spatial average, provided there are no instabilities.

Hereafter, we describe a quartz-crystal microbalance (QCM) study of the sliding of Ne monolayers on a very homogeneous Pb(111) surface at temperatures below 6.5 K, whose results are arguably the most basic evidence of the importance of commensurability in dry friction. The microbalance is a small AT-cut quartz disk whose principal faces are optically polished and covered by two lead films, which are used both as electrodes and as adsorption surfaces. By applying an ac voltage across the two electrodes, it is possible to drive the crystal to its own mechanical resonance with the two parallel faces oscillating in a transverse shear motion, characteristic of the AT cut. Because the quality factors of these modes are usually very large, on the order of 10^5, the QCM is a very sensitive probe of interfacial phenomena. A change in the inertia of the sensor, caused, for example, by the condensation of a film on the electrodes, gives rise to a shift in the resonance frequency of the normal modes, making it possible to quantify the mass of the adsorbate. Any dissipation taking place at the solid-film interface is instead detected by a decrease in the corresponding resonance amplitude [7,8].

One of the most serious problems that hinder a quantitative interpretation of the QCM data is the difficulty to accurately control the crystalline and morphological quality of the electrode surface. In most QCM studies, the morphology of the active electrode film is unknown and, in rare instances, it is determined *ex situ*. On the contrary, in this experiment it is possible, for the first time, to achieve under controlled UHV conditions the growth of the metal electrode, characterize its morphology using an ultrahigh-vacuum scanning probe microscope, and perform the QCM experiment using a specially designed setup.

The resonance frequency and amplitude are measured by means of a frequency modulation technique, in which the output signal of a radio-frequency generator is locked onto the peak resonance [9,10]. The QCM is mounted in a novel UHV system [11] that guarantees a vacuum in the

 © 2006 The American Physical Society

10^{-10} Torr range prior to the operation of the cryocooler, which improves beyond the detection limits in the sample region when the cold shields are activated. The UHV setup comprises the main chamber housing the sample holder, a fast-entry load lock system, and a UHV suitcase [12] for the transportation of the sample under vacuum conditions to the lab where the quartz electrodes are grown and characterized. The fast-entry stage is isolated by the two other parts with two gate valves and is provided with a sputtering ion gun to clean the lead electrodes from surface contaminants. A cryocooler, whose head is inserted in a specially designed jacket attached to the main chamber, is used to cool down the sample to temperatures below 10 K. The quartz is sandwiched in a specially designed mounting that provides good electrical and thermal contacts to the QCM and allows, at the same time, an easy manipulation of the QCM inside the vacuum chamber. With a wobble stick, the quartz crystal can be inserted in a copper receptacle attached to the sample holder thermally anchored to the cold finger. A film is condensed onto the QCM, kept at low temperature, by slowly leaking high-purity gas through a nozzle facing the quartz electrode.

The Pb electrodes have been grown by physical deposition using an *e*-beam heated evaporation source at a rate of 0.5 nm/ sec [13]. The evaporation is performed on a blank AT-cut quartz substrate with a resonance frequency of 5 MHz polished down to an rms roughness of about 0.3 nm. Prior to Pb evaporation, the quartz substrate was annealed under UHV conditions up to 520 K in order to remove condensed surface impurities. The deposition conditions of the lead film were carefully chosen in order to optimize the morphology of the Pb film with respect to the relevant parameters such as terrace size (step density), terrace tilt, grain size, and overall rms roughness. In order to avoid the formation of 3-dimensional clusters (Volmer-Weber growth), either elevated deposition fluxes or reduced substrate temperatures were chosen. The films used in the present QCM experiment were grown keeping the quartz substrate temperature at 155 K, and the corresponding morphology was determined *in situ* within the deposition chamber by means of STM after annealing the substrate to room temperature. Figure 1(a) shows a large scale STM image (2×2 μm^2) of a 150 nm thick Pb electrode, which reveals a distribution of polycrystalline domains with lateral dimensions around 0.5 μm. The various domains can be identified by the different stacking and orientation of the platelets. The majority of them are stacked parallel to the quartz surface, with an in-plane rotational mismatch, while a minor fraction of the platelets is stacked forming a tilt angle with respect to the substrate. An inspection of one of the domains on a closer scale is shown in Fig. 1(b). It reveals that the platelets are formed by atomic terraces, separated by monoatomic steps with a height of 0.285 nm, corresponding to the (111) termination of Pb, as shown in a more clear way by the line scans in

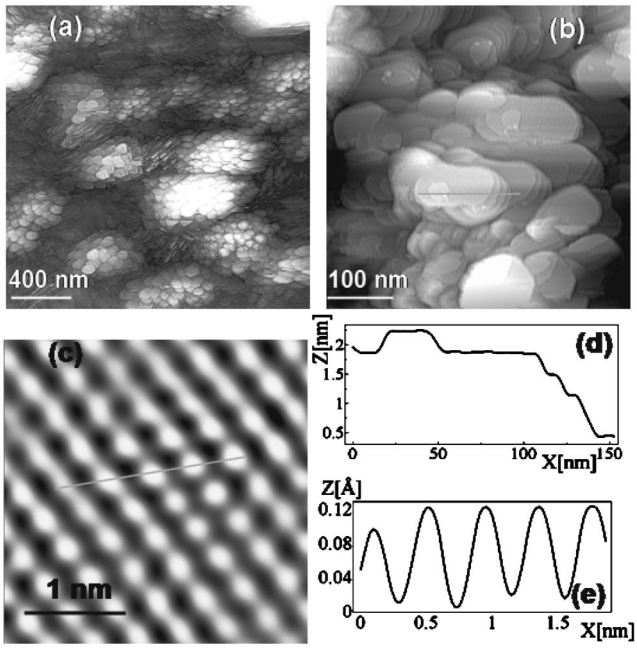

FIG. 1. (a) Large scale (2×2 μm^2) STM topography of the Pb film acquired in constant tunneling current; (b) zoomed-in view (0.46×0.46 μm^2) of the atomic planes forming a crystalline domain separated by monoatomic steps; (c) atomically resolved image (3×3 nm^2) showing the (111) symmetry of the atomic terrace; (d) line scan across the atomic terraces of (b) evidencing the step height 0.285 nm of Pb(111); (e) line scan across an atomic row evidencing the lattice spacing 0.35 nm of Pb(111).

Fig. 1(d). A more direct identification of the (111) nature of the atomic terraces and of the degree of atomic order is obtained by atomically resolved images of the terraces as those shown in Fig. 1(c) and in the line scan in Fig. 1(e), which indicates a nearest neighbor distance of 0.35 nm, again corresponding to the close packed (111) surface of lead. A statistical analysis on an extended data set allows one to extract some relevant morphological parameters: The average diameter of the crystalline grains is peaked at 480 nm, and the areal distribution of the tilt indicates that more than 85% of the exposed surface is comprised in terraces tilted less than $3° - 4°$ from the average plane, with the remaining minority fraction tilted less than 10°. The rms roughness of the film acquired on a large scale scan such as that in Fig. 1(a) corresponds to 4.5 nm, which is a remarkably low value compared to the total average film thickness of 150 nm. Finally, the terrace size distribution appears peaked around 20 nm, with a significant population of terraces as big as 90 nm. We can expect that the QCM signal will be affected mostly by the fraction of the film adsorbed on such extended, defect-free, terraces.

The two top graphs in Fig. 2 show the raw QCM data corresponding to the deposition of Ne on Pb(111) at a temperature of 6.5 K. The data have been acquired at the third overtone of a 5 MHz quartz plate characterized by a

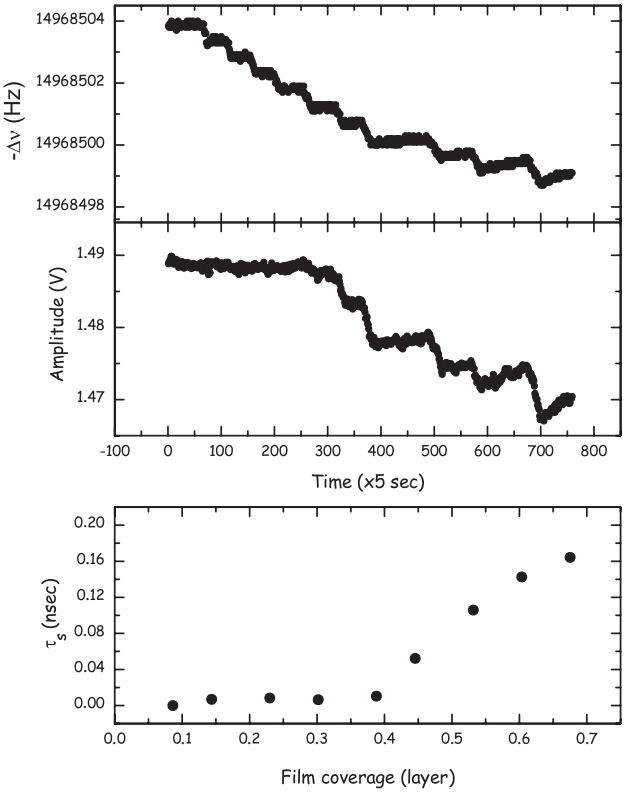

FIG. 2. Raw data of the resonance frequency shift (top) and amplitude (middle) during an adsorption isotherm of Ne on lead at 6.5 K. Bottom: Calculated slip time as a function of Ne film coverage.

quality factor of 380 000 at low temperatures. The oscillating amplitude of the quartz electrodes is estimated to be ≈ 1 nm [8]. The stability of the resonance frequency is better than ± 0.1 Hz, while that of the amplitude is ± 1 mV. For the determination of the film thickness, we have assumed an areal density for the completion of one Ne monolayer of 0.123 atoms$/\text{Å}^2$. Accordingly, the frequency shift for the deposition on one QCM electrode of a Ne layer is calculated to be equal to 7 Hz. By acting on the leak valve, the film is grown slowly in steps of about 0.1 layers and then we wait for the system to equilibrate. At low coverages, there is no change in the quartz amplitude, and only above ≈ 0.4 layers does dissipation start to appear.

This behavior is better expressed in terms of the so-called slip time τ_s [7]. Such a quantity, easily calculated from the measured frequency and amplitude shifts of the QCM, represents the time required for the adsorbed film speed to decay to $1/e$ of its initial value after the oscillating substrate has been put to rest in the absence of a bulk vapor. It varies from 0, for a film rigidly locked to the substrate, to ∞ in the case of a superfluid. The slip times described at the bottom of Fig. 2 have been normalized with film coverage according to the formulas reported in Ref. [14]. The bottom graph shows a slip time of practically zero at low coverages, while above ≈ 0.4–0.5 layers τ_s is distinctly different from zero and reaches a value of 0.3 nsec at monolayer completion, a typical value for rare gases adsorbed on metal surfaces [7,8,15]. At higher coverages, the resonance parameters are not stable over time. We believe that this behavior is due to a progressive desorption of the Ne atoms evacuated by the turbomolecular pump attached to the UHV chamber. This is the reason we could not work with the current setup at temperatures above 6.5 K and at high film coverages. In fact, the vapor pressure of solid Ne changes by 3 orders of magnitude between 5.5 and 7 K, with $P = 10^{-10}$ Torr at 6.5 K. As a consequence, we could not observe what happens to friction when a superconducting lead becomes normal at $T \geq 7.2$ K, as done by other investigators who studied the slippage of N_2 films [16,17].

The data reproducibility is a key aspect in these studies [14]. Figure 3 shows the slip times measured at the same temperature $T = 6.5$ K and excitation power but in different acquisition runs. More precisely, the measurements of runs (a) were taken over a two-day period, while those of set (b) were within a week. They all share the same general features already mentioned: very small τ_s at low film coverages followed by a distinct increase above ≈ 0.4 layers. We believe that such a good reproducibility is the result of two concurrent factors. First of all, the UHV system guarantees a very clean environment. However, we have found a progressive decrease in the dissipation and, accordingly, in the slip time, over extended measurement time periods longer than about 3 weeks. In such cases, we could effectively regenerate the Pb electrode by removing surface contaminants via ion sputtering, since the substrate damage induced by ion collisions is rapidly healed by thermally activated diffusion already at room temperature. Thanks to the large diffusion coefficient of a lead surface, this process likely removes the contaminants deposited over time on the electrode without significantly altering the initial morphology. For instance, set (b) was

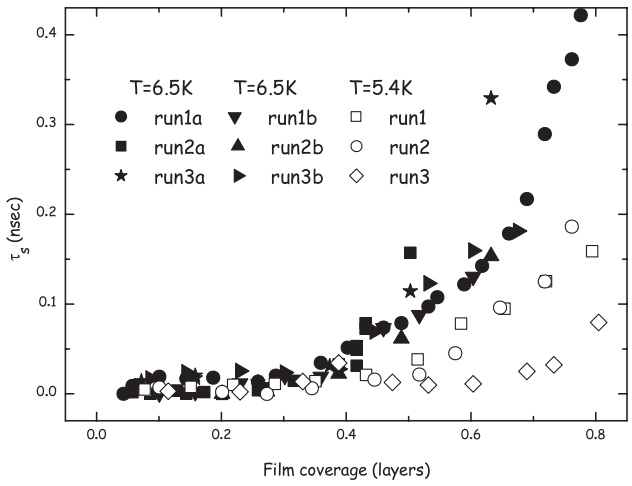

FIG. 3. Normalized slip times of Ne monolayers on lead taken at 5.4 and 6.5 K in different days. See text for further details.

taken four weeks past set (a) and after a sputtering of the QCM electrode.

Although there are no data available in the literature on the 2D phase diagram of Ne adsorbed on Pb(111), it is tempting to interpret our data in terms of a structural depinning of the film. At small coverages, the Ne film is in a fluid phase that at such low temperatures is practically locked to the substrate. Close to about 0.4 layers, some incommensurate solid islands, which are weakly bound to the surface, start to slide. This interpretation is consistent with the structural phase diagrams of heavy rare gases adsorbed on Ag(111) [18], systems that are likely not too dissimilar to Ne/Pb(111). Our measurements are also in very good qualitative agreement with the results of extensive classical molecular-dynamics simulations of a model system carried out by Persson [19] in the case of a low-corrugated substrate. Furthermore, rapid increases in τ_s near solid monolayer coverage have been recently reported for Kr adsorbed on metal(111) substrates at liquid nitrogen temperatures [15].

In particular, the numerical results show a pronounced temperature dependence of τ_s in the submonolayer region. Our data are consistent with these findings. Figure 3 compares the slip times of Ne measured at $T = 5.4$ K, the minimum temperature that it was possible to control during this experiment, with those taken at 6.5 K. Although the two temperatures are not too widely separated, the data at lower T suggest a depinning at ≈ 0.5 layers, slightly above that found at higher T, indicating that this process is thermally activated [19].

The increase in τ_s as a function of coverage shown in Fig. 3 contrasts with what some of us found studying the slippage of Kr monolayers on gold at 85 K [8,14]. We believe that this marked difference reflects the diverse pinning mechanisms involved. The Kr films were adsorbed on commercially evaporated gold electrodes, which presented a much rougher surface and smaller atomic terraces than those of the lead electrodes used in this study (see [13] for further details). Furthermore, the data on Kr/Au were taken in a conventional cryostat, where it was quite difficult to accomplish a good cleaning of the gold surfaces and where the contamination was a serious problem. In other words, the dynamics of the Kr/Au system is quite likely dominated by "extrinsic" pinning of the Kr atoms to defects present on the gold electrodes, as qualitatively seen in numerical simulations [20]. Vice versa, the Ne/Pb behavior is, in our opinion, due to "intrinsic" depinning caused by structural mismatch between the 2D islands of Ne and a very regular Pb surface.

In summary, with a quartz microbalance we have observed sliding of Ne monolayers over a lead surface at temperatures below 7 K that are suggestive of a structural depinning in agreement with recent molecular-dynamics simulations and with QCM experiments of Kr on metal(111) substrates at 77 K. Currently, we are taking extensive data with heavier adsorbates at higher T to better characterize the temperature dependence of this slip process.

It is a pleasure to acknowledge many clarifying discussions with Francesco Ancilotto, Renee Diehl, and Erio Tosatti. We thank Giorgio Delfitto for his technical assistance. This work has been supported by INFM-PRA Nanorub.

[1] See, e.g., J. Krim, Phys. World **18**, 31 (2005).
[2] R. Maboudian and C. Carraro, Annu. Rev. Phys. Chem. **55**, 35 (2004).
[3] M. Hirano and K. Shinjo, Phys. Rev. B **41**, 11 837 (1990).
[4] M. Hirano, K. Shinjo, R. Kaneko, and Y. Murata, Phys. Rev. Lett. **78**, 1448 (1997).
[5] M. Dienwiebel, G. S. Verhoeven, N. Pradeep, J. W. M. Frenken, J. A. Heimberg, and H. W. Zandbergen, Phys. Rev. Lett. **92**, 126101 (2004).
[6] A. Socoliuc, R. Bennewitz, E. Gnecco, and E. Meyer, Phys. Rev. Lett. **92**, 134301 (2004).
[7] J. Krim, D. H. Solina, and R. Chiarello, Phys. Rev. Lett. **66**, 181 (1991).
[8] L. Bruschi, A. Carlin, and G. Mistura, Phys. Rev. Lett. **88**, 046105 (2002).
[9] L. Bruschi, G. Delfitto, and G. Mistura, Rev. Sci. Instrum. **70**, 153 (1999).
[10] L. Bruschi and G. Mistura, in Nanotribology: Friction and Wear on the Atomic Scale, edited by E. Meyer and E. Gnecco (Springer, New York, to be published).
[11] L. Bruschi, A. Carlin, F. Buatier de Mongeot, F. dalla Longa, L. Stringher, and G. Mistura, Rev. Sci. Instrum. **76**, 023904 (2005).
[12] G. Firpo, F. Buatier de Mongeot, C. Boragno, and U. Valbusa, Rev. Sci. Instrum. **76**, 026108 (2005).
[13] F. Buatier de Mongeot, B. Torre, C. Boragno, and U. Valbusa (to be published).
[14] A. Carlin, L. Bruschi, M. Ferrari, and G. Mistura, Phys. Rev. B **68**, 045420 (2003).
[15] T. Coffey and J. Krim, Phys. Rev. B **72**, 235414 (2005).
[16] A. Dayo, W. Alnasrallah, and J. Krim, Phys. Rev. Lett. **80**, 1690 (1998).
[17] R. L. Renner, P. Taborek, and J. E. Rutledge, Phys. Rev. B **63**, 233405 (2001).
[18] J. Unguris, L. W. Bruch, M. B. Webb, and J. M. Phillips, Surf. Sci. **114**, 219 (1982).
[19] B. N. J. Persson, Phys. Rev. B **48**, 18 140 (1993); J. Chem. Phys. **103**, 3849 (1995).
[20] E. Granato and S. C. Ying, Phys. Rev. B **69**, 125403 (2004).